J Bioenerg Biomembr (2009) 41:343–348
DOI 10.1007/s10863-009-9237-3

NMR solution structure of the N-terminal domain of subunit E ($E_{1–52}$) of A_1A_O ATP synthase from *Methanocaldococcus jannaschii*

Shovanlal Gayen · Asha M. Balakrishna · Gerhard Grüber

Received: 18 August 2009 / Accepted: 20 August 2009 / Published online: 17 September 2009

Abstract The N-termini of E and H of A_1A_O ATP synthase have been shown to interact and an NMR structure of N-terminal $H_{1–47}$ has been solved recently. In order to understand the E-H assembly and the N-terminal structure of E, the truncated construct $E_{1–52}$ of *Methanocaldococcus jannaschii* A_1A_O ATP synthase was produced, purified and the solution structure of $E_{1–52}$ was determined by NMR spectroscopy. The protein is 60.5 Å in length and forms an α helix between the residues 8–48. The molecule is amphipathic with a strip of hydrophobic residues, discussed as a possible helix-helix interaction with neighboring subunit H.

Keywords Archaea · A_1A_O ATP synthase · ATP synthase · NMR · Subunit E · *Methanocaldococcus jannaschii*

Abbreviations

DSS, 2	2-dimethyl-2-silapentane-5-sulphonate
DTT	dithiothreitol
EDTA	ethylenediaminetetraacetic acid
HSQC	heteronuclear single quantum coherence
IPTG	isopropyl-β-D-thio-galactoside
NMR	nuclear magnetic resonance
NOE	nuclear Overhauser effect
NOESY	NOE spectroscopy
NTA	nitrilotriacetic acid
PAGE	polyacrylamide gel electrophoresis
PCR	polymerase chain reaction
RMSD	root mean square deviation
SDS	sodium dodecyl sulfate
Tris	Tris-(hydroxymethyl) aminomethane

Electronic supplementary material The online version of this article (doi:10.1007/s10863-009-9237-3) contains supplementary material, which is available to authorized users.

S. Gayen · A. M. Balakrishna · G. Grüber (✉)
School of Biological Sciences,
Nanyang Technological University,
60 Nanyang Drive,
Nanyang 637551, Singapore
e-mail: ggrueber@ntu.edu.sg

Introduction

Archae-type ATP synthases (A_1A_O ATP synthase) synthesize adenosine diphosphate and inorganic phosphate to adenosine triphosphate using an electrochemical ion-gradient (Müller and Grüber 2003; Pisa et al. 2007). The overall structure of A_1A_O ATP synthase can be divided into a cytoplasmic A_1 domain that catalyzes ATP synthesis and an integral membrane part, A_O, that serves as an ion channel (Lolkema et al. 2003; Wilkens 2005; Grüber and Marshansky 2008). The A_1 sector is elongated, with an A_3:B_3 headpiece, in which catalysis takes place and an elongated stalk (Grüber et al. 2000), composed by the subunits C, D, and F (Grüber and Marshansky 2008). Two and three dimensional reconstructions of the A_1A_O ATP synthase, obtained by single particle analysis, revealed two peripheral stalks, and a collar-like structure (Lolkema et al. 2003; Coskun et al. 2004; Bernal and Stock 2004; Vonck et al. 2009), proposed to be composed of the subunits H, E and *a*, respectively (Grüber and Marshansky 2008; Schäfer et al. 2006). Both the peripheral stalks and the collar-like structure are believed to be involved in constituting the stator region of the enzyme, which is predicted to have important roles in enzyme assembly as well as energy coupling between A_1 and A_O (Schäfer et al. 2006). The low resolution structure of subunit H of the A_1A_O ATP synthase from *Methanocaldococcus jannaschii* has been determined from small angle X-ray scattering data (Biukovic et al.

2007). Subunit H is dimeric in solution (Biukovic et al. 2007, 2009) and has a boomerang-like shape, which is divided into two arms of 120 Å and 60 Å in length (Biukovic et al. 2007). An NMR solution structure of the 60 Å long N-terminal arm, composed of the N-terminal residues 1–47 and called H_{1-47}, has been solved, revealing an α-helical feature (Biukovic et al. 2009). NMR titration and fluorescence correlation spectroscopy experiments described, that H_{1-47} interacts with the N-terminal segment of subunit E (Gayen et al. 2008) via a proposed helix-helix formation (Biukovic et al. 2009; Gayen et al. 2008). The association of subunits E and H is an important factor in the stabilization and formation of the stator in A-ATP synthases (Grüber Grüber and Marshansky 2008; Vonck et al. 2009; Schäfer et al. 2006; Gayen et al. 2008; Kish-Trier and Wilkens 2009; Esteban et al. 2008). So far the crystallographic structure of the C-terminal part (residues 81 –198) of subunit E of the A-ATP synthase from *Pyrococcus horikoshii* OT3 has been reported, showing the C-terminal domain of E composed of four antiparallel β-strands and six α-helices (Lokanath et al. 2007). In this structure the N-terminal domain was not observed. Here, we describe the production, purification and structural studies of the N-terminal part of E subunit, E_{1-52} of the A_1A_O ATP synthase from *M. jannaschii* in solution using nuclear magnetic resonance spectroscopy. Based on the E_{1-52} structure the residues involved in E-H assembly are discussed.

Experimental procedures

Biochemicals

ProofStart™ DNA Polymerase and Ni^{2+}-NTA-chromatography resin were received from Qiagen (Hilden, Germany); restriction enzymes were purchased from Fermentas (St. Leon-Rot, Germany). Chemicals for gel electrophoresis were received from Serva (Heidelberg, Germany). Bovine serum albumin was purchased from GERBU Biochemicals (Heidelberg, Germany). $(^{15}NH_4)_2SO_4$ was purchased from Cambridge Isotope Laboratories (Andover, U.S.A.). All other chemicals were at least of analytical grade and received from BIOMOL (Hamburg, Germany), Merck (Darmstadt, Germany), Roth (Karlsruhe, Germany), Sigma (Deisenhofen, Germany), or Serva (Heidelberg, Germany).

Production and purification of E_{1-52}

The gene, encoding the sequence of E_{1-52} construct, was amplified using the primers 5'- GTT GCC ATG GCT GTG AAA TTG ATG GGA - 3' (forward primer) and 5' TGC GAG CTC TCA TAT CTC TGC CTT TCT 3' (reverse primer), whereby the N-terminal construct E_{1-100} from *M. jannaschii* was used as the template (Gayen et al. 2008). The PCR product was ligated into the pET9d1-His_3 (Grüber et al. 2002) and the transformants were selected on Luria-Bertoni agar plates containing 30 μg/ml kanamycin. The recombinant E_{1-52} was produced in *E. coli* cells (BL21), which were harvested at 7 000 x *g* for 15 min at 4°C and lysed on ice by sonication for 3×1 min in buffer 1 (50 mM HEPES, pH 7.0, 150 mM NaCl, 1 mM PMSF and 0.8 mM DTT). The lysate was incubated for 20 min at 70°C and centrifugated at 10 000 x *g* for 35 min. The supernatant was filtered (0.45 μm; Millipore) and passed over a 3 ml Ni^{2+}-NTA resin column to isolate E_{1-52} (Grüber et al. 2002). The His-tagged protein was allowed to bind to the matrix for 1.5 h at 4°C and eluted with an imidazole-gradient in buffer 1. Fractions containing E_{1-52} were identified by SDS-PAGE (Laemmli 1970), pooled and applied on an ion-exchanger ResourceQ (6 ml, GE Healthcare) and equilibrated in buffer 2 (50 mM HEPES, pH 7.0, 1 mM PMSF and 1.0 mM DTT). The protein was eluted by a linear gradient with buffer 3 (50 mM HEPES, pH 7.0, 1 M NaCl, 1 mM PMSF and 1.0 mM DTT) and concentrated using Centricon YM-3 spin concentrators (Millipore). For the production of uniformly labeled (^{15}N and $^{15}N/^{13}C$) E_{1-52}, the expressing bacteria were grown in M9 minimal medium containing $^{15}NH_4Cl$ or $^{15}NH_4Cl/^{13}C$glucose. The purity of protein samples were analyzed by SDS-PAGE (Laemmli 1970). SDS-gels were stained with Coomassie Brilliant Blue G250. Protein concentrations were determined by the bicinchoninic acid assay (BCA; Pierce, Rockford, IL. USA).

NMR data collection and processing

The NMR sample was prepared in 90% H_2O/10% D_2O containing 25 mM NaH_2PO_4/Na_2HPO_4/ (pH 6.5), 0.1% NaN_3 and 60% TFE-d3. All NMR experiments were performed at 35°C on a Bruker Avance 600 MHz spectrometer. The experiments recorded on $^{15}N/^{13}C$-labelled sample were ^{15}N HSQC, HNCACB, CBCA(CO)NH and 3D ^{15}N-NOESY-HSQC (mixing time=200 ms). The proton chemical shift was referenced to the methyl signal of DSS (2, 2-dimethyl-2-silapentane-5-sulphonate). The ^{13}C and ^{15}N chemical shifts were referenced indirectly to DSS. All the NMR spectra were processed either using nmrPipe/nmrDraw (Delaglio et al. 1995) or Bruker Avance spectrometer in-built software Topspin. Spectrum analysis was performed with SPARKY program (Goddard and Kneller 1997).

NMR Spectroscopy and Structure Calculation

The additional residues of the terminal His-tag were not used in the structure calculation. Assignments were done using ^{15}N NOESY-HSQC (mixing time 200 ms) and triple-

resonance backbone experiments (HNCACB, CBCA(CO)NH). Proton side chain assignments were made using HCCCONH. The distance restraints for the structure calculation were collected from 3D ^{15}N-^{1}H NOESY-HSQC by manual assignment. The secondary structures were predicted from the chemical shift index (CSI) and NOE pattern. The upper bound for all NOE distance restraints was initially set to 5.5 Å and adjusted for nonstereospecifically assigned methylene and methyl protons using the method described originally for DYANA (Güntert et al. 1997). The structure calculation was performed with the CYANA 2.1 program package (Güntert et al. 1997). The program MOLMOL (Koradi et al. 1996) was used to visualize the result of ensemble of minimized conformers.

Results and discussion

Production and purification of the N-terminal domain of subunit E, $E_{1–52}$

The full length E subunit of the A_1A_O ATP synthase from *M. jannaschii* is composed of 206 amino acids, divided into a predicted α-helix at the N-terminal part and an α-helical and β-sheet containing domain at the C-terminal part (residues 96–206) (Lokanath et al. 2007). As the N-terminal segment of subunit E has been shown to assemble with the $H_{1–47}$ the construct $E_{1–52}$, containing the N-terminal first 52 residues, was designed for NMR structural studies. The SDS-PAGE of the recombinant $E_{1–52}$ protein revealed a prominent band of about 6 kDa, which was found entirely within the soluble fraction. A Ni^{2+}-NTA resin column and an imidazole-gradient (10–300 mM) in buffer 1 was used. The elution fractions from the Ni^{2+}-NTA purification containing the $E_{1–52}$ were collected and subsequently applied to an ion-exchanger column. Analysis of the isolated proteins by SDS-PAGE revealed the high purity of the truncated subunit.

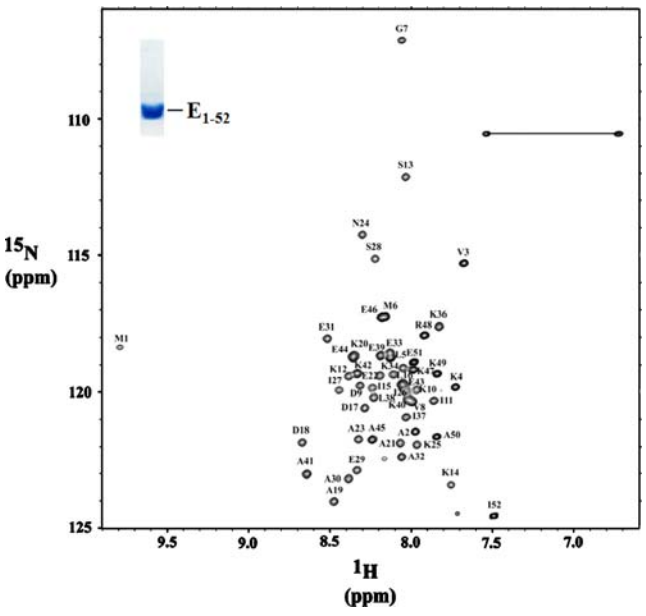

Fig. 1 ^{1}H-^{15}N HSQC spectrum of $E_{1–52}$ of the *M. jannaschii* A_1A_O ATP synthase in 25 mM sodium phosphate buffer (pH 6.5) at 308 K. Backbone and side chain (*sc*) amide assignment is shown as line for residue N_{24}. (*Insert*) SDS gel showing the sample of purified $E_{1–52}$

Table 1 Statistics for the 20 final structural models of $E_{1–52}$

Total number of NMR restraints	545
Intraresidual (|i–j|=0)	169
Sequential (|i–j|=1)	152
Short range (|i–j|≤ 1)	321
Medium-range (2 ≤|i–j|≤ 5)	146
Long-range (|*i*–*j*| > 5)	0
Dihedral angle constraints	78
Total number of restraint violations > 0.3 Å	0
Ramachandran plot statistics (%)	
Residues in most favoured regions	91.4
Residues in additionally allowed regions	8.6
Residues in generously allowed regions	0
Residues in disallowed regions	0
Average RMSD to mean (Å)	
Backbone (residues 8–48)	0.44±0.17 Å
Heavy atoms (residues 8–48)	1.10±0.17 Å

Resonance assignment of $E_{1–52}$

Assignment for the backbone HN, N, C^{α}, C^{β} and C′ resonances of the $E_{1–52}$ was achieved by a combined analysis of the triple resonance HNCACB, CBCA(CO)

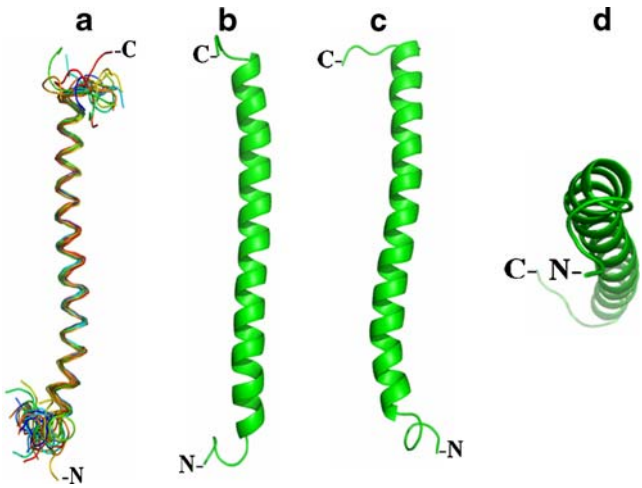

Fig. 2 Ribbon diagram of $E_{1–52}$. **a** Best fit superimposition of the 20 lowest-energy NMR structures. Side views **b**, **c** and top view **c** of the average structure of $E_{1–52}$

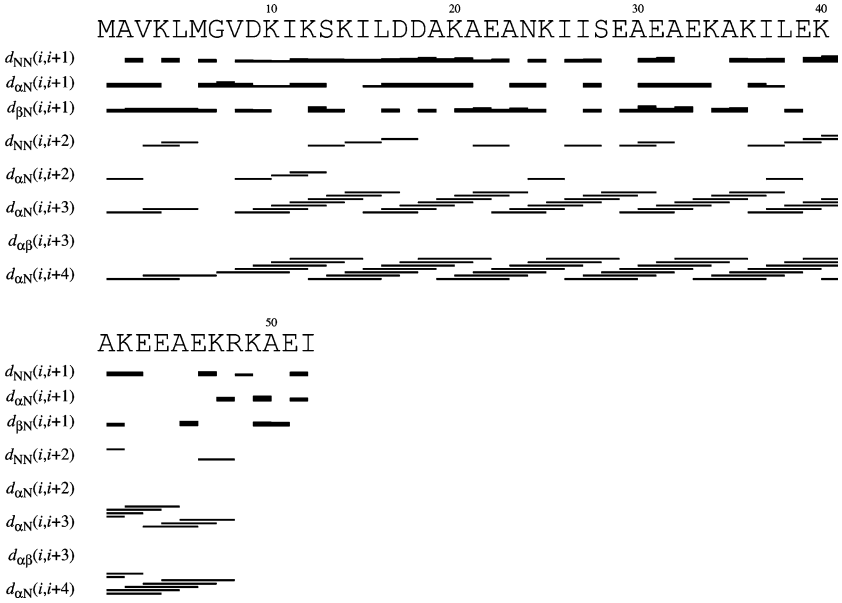

Fig. 3 Summary of structurally important NOE connectivities derived from CYANA (Güntert et al. 1997)

NH, and HNCO spectra. Figure 1 shows the good quality of the assigned HSQC spectrum indicating backbone HN and ^{15}N cross peaks of all residues of the $E_{1–52}$. Overall, the limited chemical shift dispersion of only ~ 2.0 ppm for the amide proton resonances (Fig. 1) may indicate predominantly helical conformations of $E_{1–52}$ as shown for other helical proteins (Girvin et al. 1998; Taylor et al. 2000).

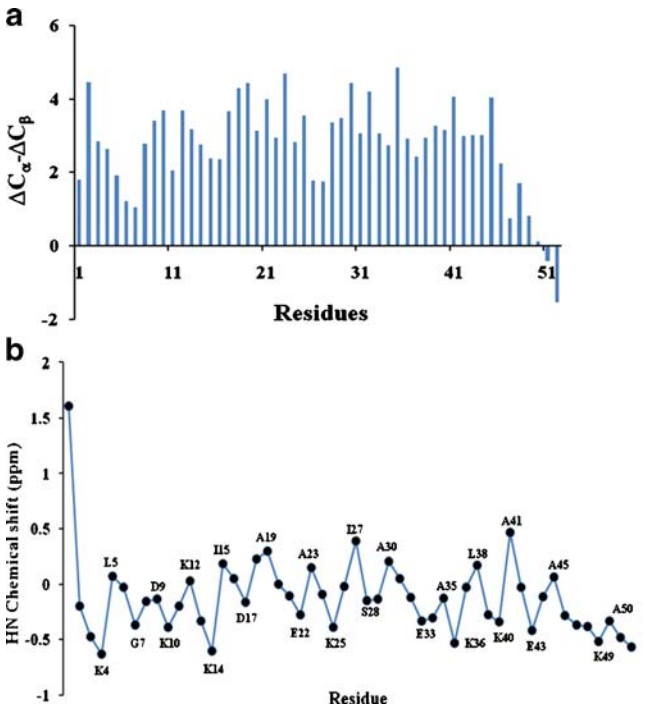

Fig. 4 **a** The amino acid sequence of $E_{1–52}$ and the secondary structure elements based on $^{13}C^{\alpha}$-$^{13}C^{\beta}$. **b** Secondary chemical shifts for NH protons for $E_{1–52}$ plotted against the residue sequence number for the $E_{1–52}$

NMR derived 3-dimensional structures of $E_{1–52}$

A total of 545 inter-proton distance restraints (169 were intraresidual, 152 were sequential and 146 were medium range) were used in the structure calculation of $E_{1–52}$, respectively, by molecular dynamics and simulated annealing (Table 1). From 100 calculated structures, 20 with the lowest total energy were selected and used for structural analysis. Figure 2a represents an overlay of the 20 lowest-

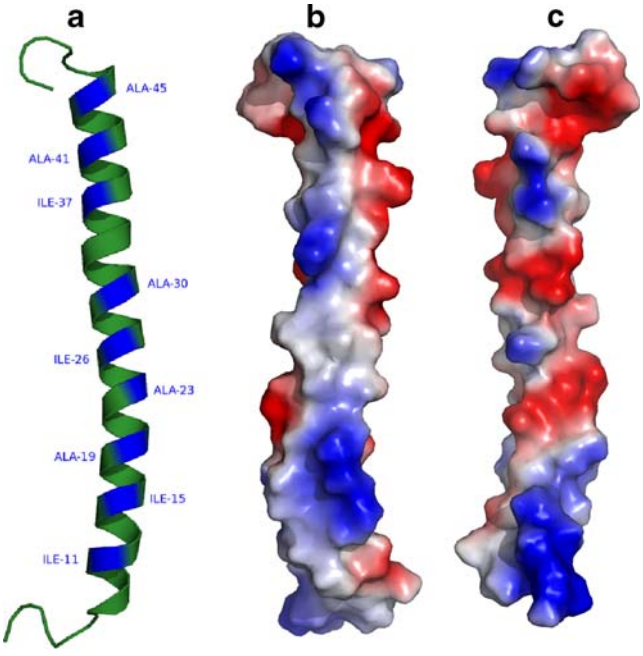

Fig. 5 **a** Ribbon representation of $E_{1–52}$ showing the hydrophobic amino acids colored in blue. **b**, **c** Surface representation of $E_{1–52}$. Red and blue represent negatively and positively charged areas, respectively, calculated with the program *pymol* (http//www.pymol.org)

energy structures of $E_{1–52}$ and the statistics are given in Table 1. A bar diagram summarizing the backbone and the backbone/sidechain NOE connectivities of $E_{1–52}$ is shown in Fig. 3. The 20 structures have an overall RMSD of 0.44 Å for backbone atoms and 1.10 Å for all heavy atoms in the helical regions (8–48) of the three dimensional structures of the protein. Figure 2b-d shows the solution structure of $E_{1–52}$ in different orientations. The protein adopts a regular α-helical conformation extending from residues Val8 to Arg48. The helical conformation is not straight, rather its N-terminal part (residues Val8-Ile26) and C-terminal part (Ile27-Arg48) are slightly bend at opposite directions (Fig. 2b-d). NH secondary chemical shifts of $E_{1–52}$, showing a 3–4 residue periodicity (Fig. 4b), support the existence of helix curvature consistent with many amphipathic and/or curved α-helices (Wagner et al. 1983; Kuntz et al. 1991; Nielsen et al. 1996; Zhou et al. 1992). The curvature of helix is caused by the differences in the H-bonding on opposite faces of the helix. Short H-bonds are correlated with low-field shifts, observed for residues Lys10, Lys14, Asp17, Glu22, Lys25, Glu29, Glu33, Lys36, Lys40 and Glu43 and long H-bonds with shifts to higher field are observed for residues Asp9, Lys12, Ile15, Ala19, Ala23, Ile27, Ala30, Ala35, Leu38, Ala41 and Ala45. The highest bending angles calculated from local helix axes fitted to CA atoms of ((i-3) - i) and (i - (i+3)) is in the region of Lys10-Ser13 using HELANAL algorithm (Kumar and Bansal 1996) (supplementary Table S1). This is further supported by the observation of $d_{\alpha N(i,i+2)}$ NOE connectivities (Fig. 3) near the N-terminus of the helix Asp9–Lys12 and Asn24–Lys25, indicating fraying or a turn at this end of the α-helix. All the structures have energies lower than—4 kcal·mol^{-1} calculated by GROMOS force field as implemented in SwissPDB viewer (Guex and Peitsch 1997). There are no NOE violations greater than 0.5 Å and no dihedral violations greater than 5°. Analysis of the Ramachandran plots shows 91.4% residues in the most favored regions, 8.6% in the additionally allowed regions. In the solution structure, $E_{1–52}$ has a total length of 60.5 Å. $^{13}C\alpha$ and $^{13}C\beta$ chemical shifts depend on local backbone geometry. Their deviations from random coil values, termed secondary shifts, provide sensitive probes to detect the secondary structural propensities. The combined carbon ($\Delta^{13}C^{\alpha}$-$\Delta^{13}C^{\beta}$) secondary shifts of $E_{1–52}$ as a function of the protein sequence (Fig. 4) show a continuous stretch of positively combined carbon secondary shifts for almost all the residues. The middle of the protein (residues 8–48) appears to have higher positive values demonstrating the presence of a helical structure in the region. The helical domain of $E_{1–52}$ presents the structural characteristics of an amphipathic helix (Fig. 5b, c) with the hydrophobic residues Ile11, Ile15, Ala19, Ala23, Ile26, Ala30, Ile37, Ala41 and Ala45 facing one side and the hydrophilic amino acids Asp9, Lys10, Lys14, Asp17, Lys20, Lys25, Glu29, Glu31, Lys36, Glu39, Glu43 and Lys47 making the second face of the helix. Using electrophoresis and mass spectrometry an E-H complex has been described. More recently, NMR titration and fluorescence correlation experiments revealed that the N-terminal part $E_{1–100}$ of subunit E of the A_1A_O ATP synthase from *M. jannaschii* assembles with residues in the N-terminal $H_{1–47}$ (Gayen et al. 2008). Together with the α-helical NMR structure of $H_{1–47}$ (Biukovic et al. 2009) and the α-helical content of $E_{1–100}$ from *M. jannaschii* (Gayen et al. 2008), derived from CD-data, it has been discussed that the assembly of both N-termini might be possible due to an helix-helix interaction of the termini of E and H (Biukovic et al. 2009; Gayen et al. 2008). As observed by circular dichroism spectroscopy, Trier and Wilkens (Kish-Trier and Wilkens 2009) discussed that truncated forms of subunit E and H, $E_{2–83}$ and $H_{2–91}$, from *Thermoplasma acidophilum* A_1A_O ATP synthase form a coiled coil interaction, reflected by molar ellipticity values at 208 nm and at 222 nm in a ratio close to 0.99. The solved NMR structure of $E_{1–52}$ with its hydrophobic strip in the α helical segment between residues 8–48, shown in Fig. 5a, forms a perfect surface for an hydrophobic and helix-helix interaction between subunit E and H and the periodicity of Ala and/or Ile residues may indicate a coiled-coil interaction of both proteins.

Acknowledgement This research was supported by A*STAR Biomedical Research Council (08/1/22/19/576). Shovanlal Gayen is grateful to the Nanyang Technological University for awarding research scholarship. Chemical shifts were submitted in BMRB (No. 16354) and the coordinates of $E_{1–52}$ have been deposited in the Protein data bank with code 2kk7.

References

Bernal RA, Stock D (2004) Structure 12:1789–1798
Biukovic G, Rössle M, Gayen S, Mu Y, Grüber G (2007) Biochemistry 46:2070–2078
Biukovic G, Gayen S, Pervushin K, Grüber G (2009) Biophysical J 97:286–294
Coskun Ü, Chaban YL, Lingl A, Müller V, Keegstra W, Boekema EJ, Grüber G (2004) J Biol Chem 279:38644–38648
Delaglio F, Grzesiek S, Vuister G, Zhu G, Pfeifer J, Bax A (1995) J Biomol NMR 6:277–293
Esteban O, Bernal RA, Donohoe M, Videler H, Sharon M, Robinson CV, Stock D (2008) J Biol Chem 283:2595–2603
Gayen S, Balakrishna AM, Biukovic G, Yulei W, Hunke C, Grüber G (2008) FEBS J 275:1803–1812
Girvin ME, Rastogi VK, Abildgaard F, Markley JL, Fillingame RH (1998) Biochemistry 37:8817–8824
Goddard T, Kneller D (1997) SPARKY 3. University of California, San Francisco
Grüber G, Marshansky V (2008) BioEssays 30:1096–1109
Grüber G, Svergun DI, Coskun Ü, Lemker T, Koch MHJ, Schägger H, Müller V (2000) Biochemistry 40:1890–1896

Grüber G, Godovac-Zimmermann J, Link TA, Coskun Ü, Rizzo VF, Betz C, Bailer SM (2002) Biochem Biophys Res Comm 298:383–391
Güntert P, Mumenthaler C, Wüthrich K (1997) J Mol Biol 273:283–298
Guex N, Peitsch MC (1997) Electrophoresis 18:2714–2723
Kish-Trier E, Wilkens S (2009) J Biol Chem 284:12031–12040
Koradi R, Billeter M, Wüthrich K (1996) J Mol Graph 14:51–55
Kumar S, Bansal M (1996) Biophys J 71:1574–1586
Kuntz ID, Kosen PA, Craig EC (1991) J Am Chem Soc 113:1406–1408
Laemmli U (1970) Nature 227:680–685
Lolkema JS, Chaban Y, Boekema EJ (2003) J Bioenerg Biomembr 35:323–336
Lokanath NK, Matsuura Y, Kuroishi C, Takahashi N, Kunishima N (2007) J Mol Biol 366:933–944
Müller V, Grüber G (2003) Cell Mol Life Sci 60:474–494
Nielsen KJ, Hill JM, Anderson MA, Craik DJ (1996) Biochemistry 35:369–378
Pisa KY, Huber H, Thomm M, Müller V (2007) FEBS J 277:56–63
Schäfer I, Rössle M, Biuković G, Müller V, Grüber G (2006) J Bioenerg Biomembr 38:83–92
Taylor RM, Zakharov SD, Heymann JB, Girvin ME, Cramer WA (2000) Biochemistry 39:12131–12139
Vonck J, Pisa KY, Morgner N, Brutschy B, Müller V (2009) J Biol Chem 284:10110–10119
Wagner GA, Pardi A, Wüthrich K (1983) J Am Chem Soc 105:5948–5949
Wilkens S (2005) Adv Protein Chem 71:345–382
Zhou NE, Zhu BY, Sykes BD, Hodgers RS (1992) J Am Chem Soc 114:4320–4326